Correspondence

The Microwave Properties of Adhesively Bonded Aluminum Foil Seams

Various interests prompted the electrical evaluation of adhesively bonded aluminum foil seams at microwave frequencies. Since epoxy resin adhesives are virtually free of volatile constituents, they are ideally suited to this application because of the vapor proof metallic boundaries confining the adhesive film. A general purpose aluminum foil of one mil thickness was used for all tests, whereas the two epoxy adhesives consisted of a conventional formulation and a silver particle filled modification.

The foil overlaps ranged from $\frac{1}{8}$ inch to $\frac{1}{2}$ inch in $\frac{1}{8}$ inch steps. Accordingly, four different samples per adhesive were available for study of the effects of variation of abutting surfaces comprising the glued joint. The cross-sectional assembly of a circular test sample is illustrated in detail in Fig. 1. The insertion of this sample is measured through its use as a closing surface of a cylindrical resonant cavity.

The span of foil overlaps develops standing waves ranging from 0.06 wavelength to 0.60 wavelength, dependent on the frequency of the electric currents traversing the seam and the depth of the seam. A frequency interval of 4.50 to 9.90 GHz was used for all tests.

The electrical data were collected through use of a cylindrical resonant cavity two inches in diameter and two inches high, which through change of mode of excitation yields not only the frequency coverage desired but also field patterns that readily permit a mathematical translation of experimental data to the required numerical results. Samples were so disposed that the adhesively bonded seams always are transversely oriented to the direction of current flow and at a location where currents attain maximum values for each mode of cavity excitation. The disturbing effects which a seam introduces within the cavity is then interpreted through precision measurement of resonant frequency as well as the attendant cavity Q. Since a sample seam is introduced through substitution of one of the inner surfaces of a cavity, its effect is readily detected by comparison of the cavity properties when resonated with an identical, but seamless, inner surface made of the same foil material as was introduced with the adhesively joined configuration of a previous measurement. The changes in cavity Q under certain test conditions are quite small, and the frequency shifts are even smaller so that the precision of frequency measuring equipment assumes much significance.

The circular samples illustrated in Fig. 2 provide the closing surfaces for the cylindrical cavity illustrated in Fig. 3. The bonded seams

Manuscript received November 5, 1965; revised September 12, 1966.

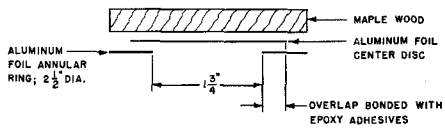

Fig. 1. Circular bonded foil sample.

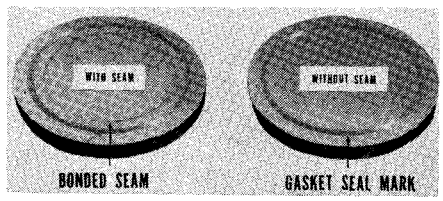

Fig. 2. Test samples for cylindrical cavity.

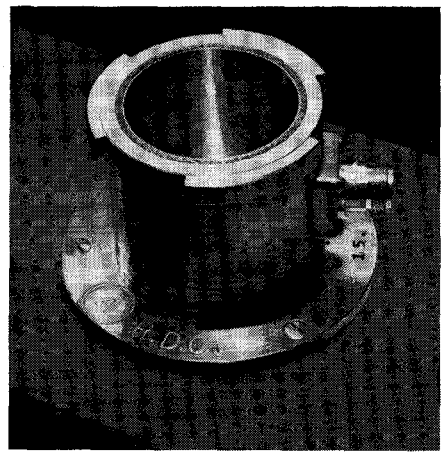

Fig. 3. Gold plated cylindrical cavity: 4.50, 5.40, 7.50, and 9.90 GHz.

are introduced at constant radius and they follow a periphery which not quite meets the vertical walls of the cavity. Fortunately, this path of bonded seam is common to the location of maximum current density of all four excitation modes. These resonant modes are designated E010, E011, E021, and E031. Excitation and identification of these various resonances are quite easily realized and they yield the following respective frequencies: 4.50, 5.40, 7.50, and 9.90 GHz. In order to evaluate R_s, the resistance per unit length of seam, and recognizing the measured loss tangent to be the sum of two contributing quantities, one may write

$$\tan\delta\ (\text{measured}) = \tan\delta_0 + \frac{\text{introduced watts}}{\omega \times \text{energy stored}} \quad (1)$$

where

$\tan\delta_0$ = dissipation factor of the cavity without an adhesively bonded seam;

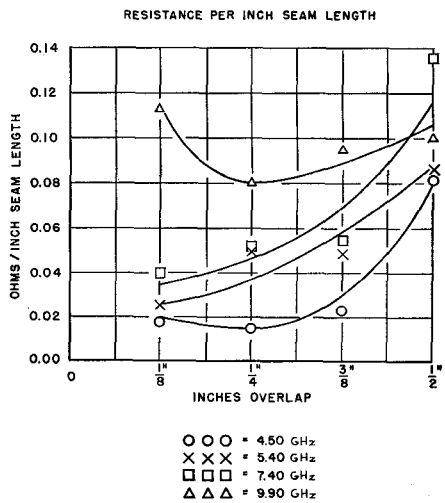

Fig. 4. Silver loaded epoxy adhesive.

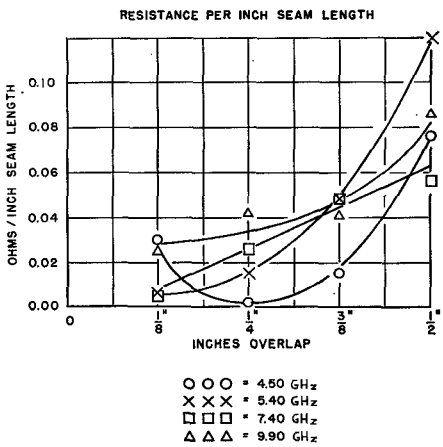

Fig. 5. Plain epoxy adhesive.

and designating

$$\tan\delta_{(\text{measured})} - \tan\delta_0 = \Delta\tan\delta \quad (2)$$

(1) and (2) may be combined to yield

$$\left[\frac{\omega\epsilon_0 a J_1\left(\frac{r_{01}}{a}r\right)}{\sqrt{2}\,r_{01}}\right]^2 2\pi a R_s = (\Delta\tan\delta)\frac{\omega\epsilon_0\pi^2a^2}{4\beta_{01}}\left[1 + a^2\left(\frac{\beta_{01}}{r_{01}}\right)^2\right] J_1^2\left(\frac{r_{01}}{a}r\right) \quad (3)$$

where the desired quantity R_s is defined in terms of ohms/meter of distance along the seam. The other symbols represent the usual quantities associated with resonance phenomena of a cylindrical cavity. In particular,

a=cavity radius, β_{01}=propagation constant associated with the E_{01} mode, and $r_{01}=2.405$, a well-known root of the Bessel function. Using E_{011} resonance constants wherever possible, R_s may be defined through (3) as

$$R_s = 544\ (\Delta \tan \delta)\ \text{ohms/inch of seam.} \quad (4)$$

Equation (4) correlates the seam resistance per unit length to the change of cavity loss tangent.

Application of well-known constants associated with other resonance modes within a cylindrical cavity then yields the required evaluations of R_s for the four resonant frequencies:

	Cavity Mode	Frequency
R_s= 900 (Δ tan δ) ohms/inch	E010	4.50 GHz
R_s= 544 (Δ tan δ) ohms/inch	E011	5.40 GHz
R_s= 756 (Δ tan δ) ohms/inch	E021	7.50 GHz
R_s=1000 (Δ tan δ) ohms/inch	E031	9.90 GHz

The resistive insertion effects generated by silver dust filled epoxy adhesives are graphically illustrated in Fig. 4 whereas the data obtained from plain epoxy adhesive seams are plotted in Fig. 5. The epoxy adhesive alone processes a measured dielectric constant value of 2.80 and a loss tangent value of 0.02 over the frequency range considered.

The reactive effects generated by plain epoxy seamed joints were typically observable through resonant frequency shifts of the order of 0.025 percent on a 2 by 2 inch cylindrical cavity. Relating this frequency shift to change of stored energy through perturbation theory, the film thickness of the plain epoxy adhesive bond computes to be 0.00034 inch (0.34 mil), which is quite reasonable for the type of assembly studied.

Conclusions

1) Aluminum foil seams bonded with plain epoxy adhesives possess a lower insertion loss than seams bonded with equivalent silver particle filled adhesives. The absence of roughness, current turbulence, and sundry discontinuity effects which are met by the passage of high-frequency currents over a dispersion of conductive particles explains to a large degree the superior behavior of the nonmetallic filled adhesive.

2) An overlap lying between $\frac{1}{8}$ and $\frac{1}{4}$ inch displays negligible insertion losses because the resistance values that are introduced through a seam within these recommended dimensions are of lesser magnitude than the high-frequency surface resistance of the basic metal foil. An optimum overlap dimension must exist; for, if the overlap is made very small, the resistance per unit length of seam must increase because of lack of area permitting the passage of current. Conversely, if the overlap is made relatively large, multiple standing waves will be introduced within the adhesive film which generate losses that necessarily increase the seam insertion resistance. Between these two intuitive extremes, there must be an optimum dimension, which is identified by these data to lie between $\frac{1}{8}$ and $\frac{1}{4}$ inch.

3) Carefully assembled adhesive joints introduce negligible reactive effects.

Werner Rueggeberg
Research and Development Center
Armstrong Cork Company
Lancaster, Pa.

Large Signal Effects in Parametric Amplifiers

It is well known that a change in pump power level usually causes a severe slope in the gain versus frequency characteristics of a parametric amplifier. A gain peak moves toward the higher end of the signal frequency band when the pump power level is increased. This is due to the increase in average capacitance of the diode with increasing the pump power level, causing a decrease in the resonant frequency of the idler circuit. To minimize this gain slope, sometimes a self bias is superimposed onto the fixed bias of the diode to cancel the change in average capacitance. This technique is successful in minimizing the effect of pump power variation on the gain slope. However, under large signal conditions (output power >-12 dBm), the average capacitance of the diode is also changed by the input signal level. Since the rectified diode current due to the large signal is much larger than that due to the pump for the same change in average capacitance, an optimum compensation bias resistance for pump power variation is too large for signal power variation. This results in an overcompensation and causes a large opposite gain slope. On the other hand, for a frequency combination where a third of the pump frequency $f_p/3$ is close to the signal band center frequency f_{sc}, a situation which corresponds to a 1:2:3 relationship of signal, idler, and pump frequencies, abnormal gain peaking at about $f_p/3$ was observed. In cases where $f_p/3$ is lower than f_{sc}, this abnormal gain peaking appears at the lower-frequency side of the band, and introduces also an opposite slope as to the normal gain slope. This makes it impossible to compensate this gain slope by a positive resistance bias circuit.

The amplifier used for investigation of these abnormal effects was operated at 3.95 GHz signal center frequency f_{sc} and 11.76 GHz pump frequency. In this case $f_p/3$ is 30 MHz below f_{sc}. For broadband gain a double tuned idler circuit was provided. Figure 1 shows the gain versus frequency characteristic of the amplifier adjusted to achieve a flat characteristic with 13 dB gain at an input power of -35 dBm. The frequency scale for these photographs is about 25 MHz/cm. For comparison reference gain and ± 1 dB lines are drawn. Figure 2 shows the characteristic for -20 dBm input. There is a gain compression at f_{sc} and a peak around $f_p/3$.

To explain this peculiar behavior, the spectrum of the amplifier output was analyzed and it was found that with increasing signal power higher-order mixing products, especially the component at the frequency $f_i-f_s=f_{i-s}$, increase very rapidly. This additional component is strongest around $f_s=f_p/3$ where the signal frequency f_s and its corresponding f_{i-s} coincide. At high-signal levels, this f_{i-s} component is only about 6 dB below the f_s component. It was also observed that with increasing signal level the peak power frequency in the f_{i-s} band shifts to the high-frequency side.

The f_{i-s} component not only adds to the signal output but creates a secondary effect: at high signal and pump levels the idler acts as a second pump for an additional degenerate amplifier mode with f_{i-s} as a second idler, thus causing additional gain for those signals whose corresponding f_{i-s} component is strong. This seems to be an important factor for introducing the peak at $f_p/3$. As the signal and the corresponding f_{i-s} are very close together around $f_p/3$, the strong component at f_{i-s} in the vicinity of $f_p/3$ also causes major additional gain at f_s around this frequency. When the f_{i-s} band broadens to the higher frequency side with increasing signal levels, the peak caused by additional degenerate gain should broaden to the lower frequency side, which was actually observed.

To justify this theory, gain measurements were made with the spectrum analyzer. Picking only the signal frequency component of the amplifier output, its gain was measured as a function of input signal level at $f_s=f_p/3$, and $f_s=f_{sc}$. This was done for 16, 13, and 10 dB gain at -20 dBm input. The results are shown in Fig. 3. There is normal compression of the signal gain at center frequency f_{sc} with increasing signal level, while it stays rather constant at $f_s=f_p/3$ from -40 to -30 dBm input and slightly *increases* at higher input signals. In the 16 dB gain case, the gain is the maximum at -25 dBm input and is compressed at -20 dBm.

Under strong pumping and high gain conditions additional nonlinear effects occur, especially in the vicinity of $f_p/3$ which are responsible for extreme gain peaks around this frequency.

Figure 4 explains these phenomena: f_s and f_{i-s} were chosen close to $f_p/3$ ($f_s=3.915$ GHz, $f_{i-s}=3.930$ GHz).

The experiment was performed by maintaining the signal input power constant at a certain level, and increasing the pump power steadily. All measurements were taken with the amplifier detuned to a higher bias value because under a large pump and signal condition the idler circuit was tuned to near $\frac{2}{3}f_p$, and it resulted in subharmonic oscillations at $\frac{2}{3}f_p$ and $\frac{1}{3}f_p$ easily. Also at lower bias voltages, the large signal nonlinear characteristics were different depending upon the operating conditions. However, all nonlinear effects observed at low bias voltages were reproduced at the higher bias voltage at which the results recorded in Fig. 4 were taken.

Figure 4(a) shows the output spectrum (f_s and f_{i-s}) of the amplifier with a finite gain at f_s. When the pump power was further increased, a sudden jump in the output of more than 20 dB at both the frequency components was observed. Also, many intermodulation products were generated, shown in Fig. 4(b). This jump is more pronounced when 1) the input signal power is low, and 2) f_s is closer to $f_p/3$. For high input signal power (e.g., >-20 dBm) there is a steep, but not sudden, increase of output with increasing pump power before oscillations start.

Well pronounced jumps were observed for input powers <-30 dBm.

When the pump power was further increased, a subharmonic oscillation appeared at $f_p/3$ knocking down the f_s and f_{i-s} components as shown in Fig. 4(c). From these observations, the "gain jump" can be explained as a result of oscillations which are controlled by the signal f_s and are completely coherent with f_s. This explanation is also backed by the

Manuscript received February 11, 1966; revised July 22, 1966.